

## Fluctuations and bubble dynamics in first-order phase transitions

Mark Abney\*

*Department of Physics, The Enrico Fermi Institute, The University of Chicago, Chicago, Illinois 60637  
and NASA/Fermilab Astrophysics Center, Fermi National Accelerator Laboratory, Batavia, Illinois 60510*

(Received 3 July 1996)

We numerically examine the effect of thermal fluctuations on a first-order phase transition in (2+1) dimensions. By focusing on the expansion of a single bubble we are able to calculate changes in the bubble wall's velocity as well as changes in its structure relative to the standard case where the bubble expands into a homogeneous background. Not only does the wall move faster, but the transition from the symmetric to the asymmetric phase is no longer smooth, even for a fairly strong transition. We discuss how these results affect the standard picture of electroweak baryogenesis. [S0556-2821(97)03602-3]

PACS number(s): 98.80.Cq, 64.60.Qb

### I. INTRODUCTION

Recent numerical and analytical work on weak first-order phase transitions has shown that there may be significant changes to the standard theory of phase transitions as a result of thermal fluctuations [1–6]. Instead of a smooth homogeneous background there may be a significant amount of phase mixing due to the existence of subcritical bubbles. Though not without controversy [7,8], these findings suggest we may need to reevaluate the standard theory of nucleation of critical bubbles because in very weak first-order phase transitions the standard assumption of only small amplitude fluctuations breaks down. As the phase transition increases in strength we expect the role of fluctuations to diminish until the approximations made for homogeneous nucleation become applicable. The effects of thermal fluctuations may extend beyond the regime of nucleation however, and alter the dynamics of bubbles as they expand. Due to the complex nature of the system, analytic investigations of this question would be difficult. On the other hand, numerical simulations in 3+1 dimensions would be very computationally extensive. We therefore address the problem of dynamics by undertaking numerical simulations in (2+1) dimensions. Our primary motivation is to gain at least a qualitative understanding of how thermal fluctuations may affect the electroweak phase transition in the early universe and the consequent ramifications on baryogenesis at this epoch.

Work on the topic of electroweak baryogenesis has, in general, been concentrated in three areas: the form of the effective potential [9], the dynamics of the transition [8, 10–14], and how to calculate the baryon asymmetry [15–20]. These three areas effectively form a hierarchical structure where the means by which one computes the baryon asymmetry depends on the dynamics of the transition, which in turn depends on the form of the effective potential. Though we do not yet know what the true effective potential looks like, it nevertheless makes sense to investigate the other two areas by assuming certain generalities. That is, we may choose a theory with a scalar order parameter  $\phi$  responsible for spontaneous symmetry breaking. If we assume a potential

which may be approximated by

$$V = a\phi^2 - b\phi^3 + c\phi^4, \quad (1)$$

where the coefficients are temperature dependent, we can compute quantities such as the temperature needed to nucleate bubbles of the new phase, the thickness of the bubble walls, and the rate at which the old phase is converted to new phase as a function of the coefficients.<sup>1</sup> We require a first-order transition because of the third of Sakharov's conditions for baryogenesis, the lack of thermal equilibrium. Because the cooling rate of the Universe is extremely slow at the electroweak transition, depending only on the rate of expansion, the cosmological fluid maintains thermal equilibrium. However, by allowing a bubble of stable vacuum to appear within the metastable vacuum, a first-order transition gives rise to out of equilibrium processes in the neighborhood of the bubble wall. It is only within this confined region where baryogenesis can take place.

The order and strength of the electroweak phase transition is the subject of ongoing research which will only be solved by a calculation of the effective potential which is valid to all orders of perturbation theory. In any case we will assume a potential of the general form of Eq. (1). The strength of the transition is determined by a ratio of the coefficients in Eq. (1), the value of which is temperature and model dependent. In the minimal standard model for the electroweak theory the quark, gauge boson, and Higgs masses determine the height of the energy barrier separating the two minima of the effective potential. If the Higgs mass is small the transition is strongly first order, whereas a large Higgs mass results in a transition which is at most weakly first order and possibly second order. While most work on phase transition dynamics has been done for a strong first order transition, the experimental lower bound on the Higgs mass of 65 GeV [21] has all but ruled out this regime in the context of the minimal standard model. More recently, there has been interest in the

<sup>1</sup>In fact, the rate of phase conversion depends on the velocity of expansion of the bubble walls, which depends not only on the strength of the transition but also on the interaction of the wall with the cosmological plasma.

\*Electronic address: abney@oddjob.uchicago.edu

dynamics of very weak first order transitions [1–6]. In this case the phase transition may be completed through the process of phase mixing, whereby subcritical bubbles effectively restore symmetry, rather than the conventional nucleation of critical bubbles. However, it is also possible that the dynamics lie in the intermediate region between a strong transition — nucleation and expansion of bubbles in a homogeneous background — and a weak transition — phase mixing and domain coarsening.

This work focuses on the dynamics of a transition which lie in this intermediate region. In this case fluctuations will not be strong enough to completely dominate the transition and restore thermal equilibrium, yet may have an effect on processes such as the nucleation and expansion of bubbles. Though we will not address the issue of nucleation (see [5–7] for discussions on this topic), we will investigate the ramifications of fluctuations on the speed and structure of the bubble wall and what the implications are on the standard mechanisms for generating excess baryons at the electroweak phase transition. These mechanisms depend strongly on particle interactions with the bubble wall, and calculating the resulting baryon abundance requires knowledge of the details of the transition, including the wall’s speed and structure. Some authors have argued that subcritical bubbles are not relevant to baryogenesis since fluctuations only have an effect when the phase transition is only very weakly first order, too weak to be of interest to baryogenesis [7,8,15]. These arguments, however, deal primarily with the question of whether the phase transition proceeds through the nucleation of critical bubbles. The issue addressed in here is whether the fluctuations can have a significant effect on critical bubbles after they nucleate.

This issue is related to one which has recently become of interest in condensed matter physics. Specifically, there has been an effort to understand how noise affects the properties of front propagation in a phase transition [22]. The results of these studies has varied depending on the specifics of the model in question. Here, though fluctuations play the role of the noise in the phase transition, the system we consider and the model we use to analyze it is significantly different from those evaluated within the context of condensed matter.

Once one understands the dynamics of the electroweak phase transition it becomes possible to calculate the baryon asymmetry. Traditionally, baryogenesis has been investigated in two different limits, thin walls or thick walls. In the thin wall regime the wall is thin compared to the mean free paths of the particles, which behave as if they were scattering off a potential barrier with  $CP$ -violating reflection coefficients. The reflected charge results in a baryon asymmetry in the region preceding the phase boundary. In the thick wall case the plasma is treated as though it were in quasistatic thermal equilibrium. Chemical potentials are introduced for quantities which vary slower than the time it takes for the bubble wall to pass, and baryogenesis is the result of a change in the  $CP$ -violating phase, which acts like a chemical potential for baryon number [17]. In both cases the transition from one vacuum state to the other is smooth, with the order parameter varying monotonically. If fluctuations play a significant role it is likely that there would be deviations away from the smooth transition model. It is unclear, though, for what transition strength these deviations can be ignored. Fur-

thermore, our assumptions about how thick the wall is for a given transition strength may have to be modified.

The plan of this article is as follows. In Sec. II we discuss the potential we use in our simulations and its temperature dependence. Section III contains the evaluation of the nucleation temperature and expansion velocity of critical bubbles in the standard homogeneous background model in (2+1) dimensions. We elaborate on our model for the phase transition with thermal fluctuations in Sec. IV, covering such issues as the equation of motion, lattice considerations, and specific results. Finally, in the conclusion, we discuss ramifications to electroweak baryogenesis as well as possible improvements for future work.

## II. THE STANDARD SCENARIO

### A. The potential

The potential we select deliberately resembles the temperature-dependent electroweak effective potential for the minimal standard model:

$$\tilde{V}(\phi, T) = \frac{a}{2}(T^2 - T_2^2)\phi^2 - \frac{\tilde{\alpha}}{3}T\phi^3 + \frac{\tilde{\lambda}}{4}\phi^4. \quad (2)$$

The parameters  $\tilde{\alpha}$  and  $\tilde{\lambda}$  determine the strength of the phase transition and in the minimal standard model are related to the gauge boson masses and the Higgs boson mass, respectively. The application of this potential, however, may be more general and useful in studies of first order transitions. Because of the (2+1)-dimensional nature of the simulations,  $\tilde{V}$  has a mass dimension of  $[M^3]$  with  $\tilde{\phi}$  being  $[M^{1/2}]$ . Furthermore, we do not associate particular values of  $\tilde{\alpha}$  and  $\tilde{\lambda}$  with particle masses, but rather concentrate on which regions of parameter space constitute weak and strong transitions as determined in Ref. [2].

We will find it useful to change from dimensional to dimensionless variables as follows:

$$x \rightarrow x/\sqrt{a}T_2, \quad (3)$$

$$t \rightarrow t/\sqrt{a}T_2, \quad (4)$$

$$\phi \rightarrow \chi T_2^{1/2}, \quad (5)$$

$$T \rightarrow \theta T_2. \quad (6)$$

The potential is now

$$V(\chi, \theta) = \frac{1}{2}(\theta^2 - 1)\chi^2 - \frac{1}{3}\alpha\theta\chi^3 + \frac{1}{4}\lambda\chi^4, \quad (7)$$

where  $\alpha = \tilde{\alpha}a^{-1}T_2^{-1/2}$  and  $\lambda = \tilde{\lambda}a^{-1}T_2^{-1}$ . For  $\theta < \theta_1 = (1 - \alpha^2/4\lambda)^{-1/2}$  the potential has one maximum  $\chi_-$  and two minima  $\chi_0, \chi_+$  located at  $\chi_0 = 0$  and  $\chi_{\pm} = \alpha\theta/2\lambda(1 \pm \sqrt{1 - 4\lambda(1 - \theta^{-2})/\alpha^2})$ . At the critical temperature  $\theta_c = (1 - 2\alpha^2/9\lambda)^{-1/2}$  the two minima are degenerate with the minimum at  $\chi_+$  being the global minimum for  $\theta < \theta_c$ . At  $\theta = 1$  the minimum at  $\chi_0$  disappears. Figure 1 shows the potential for  $\lambda = 0.1, \alpha = 0.4, \theta = \theta_c - 0.0025 = 1.2432$ .

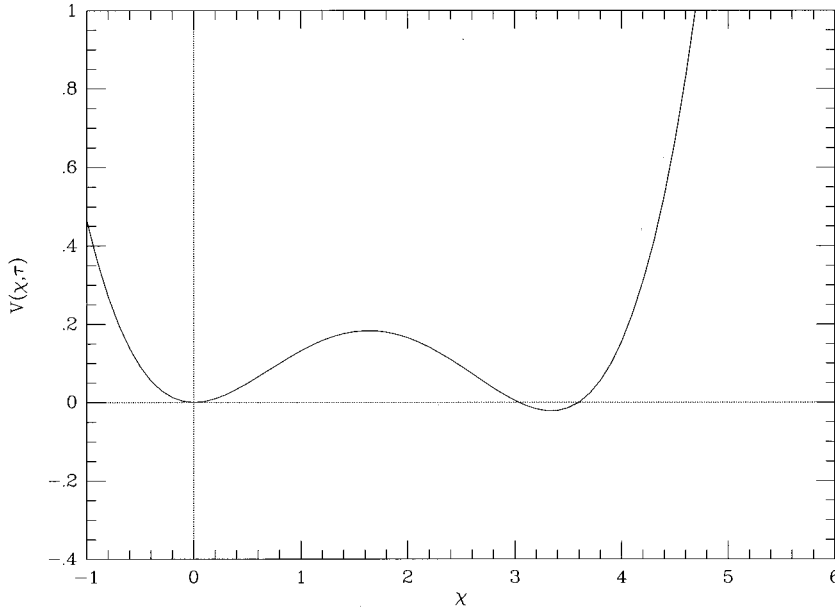


FIG. 1. Potential for  $\lambda=0.1$ ,  $\alpha=0.4$ ,  $\theta=\theta_c-0.0025=1.2432$ .

### B. Dynamics

The dynamics of the phase transition depends to a large degree on the amount of supercooling undergone before the nucleation of bubbles. If the supercooling is large, as in the case of a strong first-order transition, the bubbles expand very rapidly and have a relatively thick wall. In a weak transition the free energy of a bubble is minimized for a thin wall and the small cooling results in a slowly moving wall. The first step, then, is to determine the temperature at which nucleation takes place.

As the universe cools below the critical temperature the symmetric vacuum becomes metastable with a finite probability of decaying into the asymmetric stable vacuum. The theory of bubble nucleation from a metastable to a stable state was developed by Langer [23] and later applied to cosmological phase transitions [24,25]. The equation describing the rate of nucleation per volume in 3+1 dimensions, however, must be changed to account for the different scaling in a (2+1)-dimensional model. Recall that in two dimensions volume scales as  $T^{-2}$  and not  $T^{-3}$ . The nucleation rate per volume is

$$\Gamma/\mathcal{V}=AT^3e^{-F_c/T}, \quad (8)$$

where  $F_c$  is the free energy of a critical bubble. The rate is dominated by the exponential; hence, the exact value of  $A$  is not very important and we set it equal to one. The nucleation temperature is given by the temperature at which the probability of nucleating a critical bubble inside a horizon approaches one. We must, therefore, determine the size of the horizon as a function of temperature. In a (2+1)-dimensional universe during the radiation dominated era, the energy density of the Universe  $\rho$  varies with the scale factor  $a$  according to  $\rho \propto a^{-3}$ . The time-temperature relation is then

$$t = \xi \frac{m_{\text{Pl}}^{1/2}}{T^{3/2}}, \quad (9)$$

where  $m_{\text{Pl}}=1.22 \times 10^{19}$  GeV is the Planck mass and  $\xi \approx 1/30$  [28]. The volume inside the horizon at a temperature  $T$  is

$$\mathcal{V}_H \approx 4\xi^2 \frac{m_{\text{Pl}}^3}{T^3}. \quad (10)$$

From this we can write down the probability of nucleating a bubble inside a causal volume at a temperature  $T$ :

$$dP \approx \Gamma \mathcal{V}_H dt \approx 6\xi^2 \left(\frac{m_{\text{Pl}}}{T}\right)^{3/2} e^{-F_c/T} \frac{dT}{T}. \quad (11)$$

We define the nucleation temperature as the temperature for which the total probability of having nucleated a bubble approaches one:

$$1 \approx 4\xi^2 \left(\frac{m_{\text{Pl}}}{T_n}\right)^{3/2} e^{-F_c/T_n}, \quad (12)$$

where  $T_n$  is the nucleation temperature. Estimating  $T_n$  is made much simpler by approximating  $T_n$  in the prefactor of the right hand side of Eq. (12) as the critical temperature. Because of the exponential, the final answer is not very sensitive to the value of the critical temperature chosen. A value of  $T_c=100$  GeV yields

$$53 \approx F_c/T_n. \quad (13)$$

In order to calculate the free energy of a vacuum bubble, we choose the energy of the metastable vacuum as zero,  $V(\langle\phi\rangle=0)=0$ . The excess free energy of a bubble is

$$F = \int d^2x \left[ \frac{1}{2}(\nabla\phi)^2 + V(\phi, T) \right]. \quad (14)$$

The first term in the integral represents the surface energy of the bubble, while the second term is the volume energy, coming from the difference in free energy inside and outside the bubble. The free energy, in general, must be found numerically. The difficulty in calculating  $F$  arises because one

needs to know the value of the field at all points in space, which in general may not take a simple functional form. Under certain limits, however, approximations prove fairly accurate. In the case of extremely small supercooling the wall approaches the well-known kink solution, the ‘‘thin wall’’ approximation. As the temperature drops further below the critical temperature the wall shape is reasonably approximated by a Gaussian [10]. At temperatures appropriate to nucleation, neither approximation turns out to be particularly good. In spite of the fact that the thin wall approximation fails to accurately predict the free energy associated with the nucleation of critical bubbles, we use it here as a way of estimating a value for  $T_n$ . One should bear in mind, however, that the free energy of the true critical bubble solution is larger than the free energy in the thin wall case at a given temperature. As a result the nucleation temperature in the thin wall case is higher, i.e., less supercooling, than in the true case. We, however, are not most interested in what the actual nucleation temperature is, but rather in the dynamics of bubble expansion. Within this context the thin wall approximation gives a reasonable estimate. Also, recent studies have shown that the actual nucleation temperature may be significantly higher than what one obtains by the standard method [5,6]. The basic idea is that in a weak first-order transition large amplitude fluctuations cause the energy density of the metastable vacuum to shift away from  $V(0)$ . Instead one must include a nonperturbative correction to the free energy of a critical bubble which has the effect of raising the nucleation temperature.

To calculate the free energy in the thin wall limit, when supercooling is small, we use a perturbative expansion in  $\Delta \equiv 1 - \theta/\theta_c$ , the amount of cooling below the critical temperature. To first order the potential is

$$V(\chi, \theta) = \frac{1}{2}(\theta_c^2 - 1)\chi^2 - \frac{1}{3}\alpha\theta_c\chi^3 + \frac{1}{4}\lambda\chi^4 - \Delta\left(\theta_c^2\chi^2 - \frac{1}{3}\alpha\theta_c\chi^3\right). \quad (15)$$

A bubble of true vacuum which is just large enough to grow satisfies the static solution to the equations of motion,

$$\frac{d^2\chi}{dr^2} + \frac{1}{r}\frac{d\chi}{dr} = \frac{\partial V}{\partial\chi}. \quad (16)$$

In the thin wall limit the spatial derivatives are small except in the bubble wall. Furthermore, when  $\Delta$  is small the radius of a critical bubble becomes very large and the first order derivative term in Eq. (16) becomes negligible. This gives

$$\frac{d\chi}{dr} = \sqrt{2V}. \quad (17)$$

The free energy of a bubble of radius  $R$  is

$$F \approx \pi R \int_{\chi(R-\delta R)}^{\chi(R+\delta R)} d\chi \sqrt{2V} + 2\pi \int_0^R dr r V(\chi_+, \theta), \quad (18)$$

where  $\chi_+$  represents the value of the field of the true vacuum and is given by

$$\chi_+ \approx \frac{2\alpha\theta_c}{3\lambda} - \Delta \left( \frac{2\alpha\theta_c}{3\lambda} - \frac{6}{\alpha\theta_c} \right). \quad (19)$$

As a function of the radius  $R$  and the amount of supercooling  $\Delta$  the free energy is

$$F(R, \Delta) \approx \frac{2\pi R}{81} \sqrt{2\lambda} \left( \frac{\alpha\theta_c}{\lambda} \right)^3 - \frac{4\pi R^2}{9} \left( \frac{\alpha\theta_c}{\lambda} \right)^2 \Delta. \quad (20)$$

By taking the derivative with respect to  $R$  we get the radius of a critical bubble  $R_c = \alpha\theta_c / (18\sqrt{2\lambda}\Delta)$ . Since  $\Delta$  is small, the nucleation temperature is approximately the critical temperature, and after equating with Eq. (13) we get for the critical free energy to temperature ratio

$$\frac{F_c}{\theta_n} \approx \frac{\pi}{1458} \frac{\alpha^4\theta_c^3}{\lambda^3\Delta} \approx 53 \quad (21)$$

or

$$\Delta \approx (4.07 \times 10^{-5}) \frac{\alpha^4\theta_c^3}{\lambda^3}. \quad (22)$$

Once a critical bubble is nucleated it begins to expand because the free energy lost due to the interior being in the lower energy vacuum offsets the gain in surface energy. The wall quickly accelerates, and in the case of a vacuum transition, approaches the speed of light within a few wall widths [25]. In the more realistic case where the wall is expanding through a plasma, the wall experiences an opposing force due to interactions with particles and reaches a terminal velocity. Calculating the terminal velocity proves to be a difficult problem because it depends on detailed interactions of the Higgs field with the plasma. Furthermore, the size of the damping also depends on the thickness of the wall relative to the mean free paths of the particles in the plasma [10]. Simply, this results because a thin wall causes particles to make the transition into the true vacuum state quicker than the time it takes for them to equilibrate. A thicker wall allows the particles to maintain quasistatic thermal equilibrium, because the thermalization rate is faster than the rate at which the Higgs field changes, but not chemical equilibrium, because some particle interaction rates occur slowly resulting in departures from equilibrium populations. The result is a different damping force depending on the regime. In any case, we assume here that the damping force can be modeled by a velocity dependent term in the equation of motion of the Higgs field, where the magnitude of the proportionality constant determines the terminal velocity:

$$\frac{d^2\chi}{dt^2} + \eta \frac{d\chi}{dt} - \nabla^2\chi = -\frac{\partial V}{\partial\chi}. \quad (23)$$

In the frame moving with the wall we can change coordinates to  $\tau = \gamma(x - vt)$ , simplifying to the case of a very large bubble so that we may treat the problem as effectively one dimensional. The equation of motion then takes the form

$$\frac{d^2\chi}{d\tau^2} + \eta\gamma v \frac{d\chi}{d\tau} = \frac{\partial V}{\partial\chi}. \quad (24)$$

The boundary conditions on  $\chi$  state that the derivative must vanish far from the wall. We can then integrate to obtain

$$\eta\gamma v \int_{-\infty}^{\infty} \left( \frac{d\chi}{d\tau} \right)^2 d\tau = V(0) - V(\chi_+) \quad (25)$$

$$= -V(\chi_+). \quad (26)$$

Within the validity of the thin wall approximation, we may perform the integral analytically to obtain

$$\frac{1}{6} \eta\gamma v \sqrt{\frac{\lambda}{2}} \chi_+^3 = V(\chi_+). \quad (27)$$

Several authors [8,10,11,14] have calculated the velocity of the bubble wall in both the thick and thin case. The results for a thin wall are  $v \sim 0.1$  and  $v \sim 0.2-0.6$  for a thick wall. Given a particular set of parameters for the potential, then, we can find an appropriate value for  $\eta$ . Here we say that  $\eta$  is generally  $\sim 0.1$ .

Up to this point our treatment of the bubble has been from a purely field theoretic point of view. We describe the dynamics of the Higgs field as a scalar field in a temperature dependent potential. Particles in the plasma scatter off the field effectively creating a damping force. A more macroscopic view of the phase transition describes the plasma through hydrodynamics and the bubble wall as an effective combustion front. In this case there are several effects which arise which affect the dynamics of the bubble expansion which are not otherwise evident in the field theoretic point of view. The velocity of the wall, for instance, depends not only on the damping coefficient  $\eta$ , but also on the ability of the fluid to conduct heat away from the wall and the resulting small temperature deviations created through the release of latent heat [11,14]. Furthermore, fluid dynamical instabilities can arise both in the plasma and the bubble wall. Perturbations in the wall may grow exponentially depending on the size of the perturbation and the strength of the front [26–31]. The net effect is that bubbles might not grow in a spherically symmetric way. Nevertheless, including these effects is beyond the scope of this work and we consider here only the simplified scenario of a scalar field in a potential well with damping.

### III. PHASE TRANSITIONS WITH FLUCTUATIONS

Thermal fluctuations play an essential role in the phase transition, so it is instructive to discuss briefly how they enter into the physical picture. Without fluctuations the field remains trapped in the metastable vacuum until the potential barrier vanishes at which time the field rolls down the potential into the true vacuum. In a thermal environment, though, it is only the expectation value of the field which is in the metastable state. There is a finite probability that the field can take on a value beyond the potential barrier and thus make the transition into the true vacuum. Hence, the nucleation and expansion of bubbles. This method, however, traces the evolution of the field using the equations of motion at zero temperature often with a damping term to simulate the dissipation due to the thermal environment, with finite temperature effects limited to corrections to the effective po-

tential. This approach is justifiable if one wishes to consider only the behavior of the expectation value of the field, where one has implicitly assumed that the variance of the field value is very small. This assumption should hold if the minima in the effective potential are sufficiently deep that thermal fluctuations away from the minima are strongly suppressed. Even in this case, however, the dynamics of the field may not be adequately described by the equations of motion. For instance, if the field is initially located at a local minimum of the potential, which then becomes a local maximum in such a way that the slope remains zero, the field remains in this unstable extremum indefinitely. Realistically, what happens is that fluctuations dislodge the field from the extremum, which subsequently evolves according to the equations of motion.

The question of how one is to model the thermal fluctuations in field theory nevertheless remains. In classical statistical mechanics one treats the problem of thermal fluctuations by identifying a system and a heat bath and choosing a model for the coupling between the two and solving for the behavior of the system. Finding a solution is greatly simplified when the reservoir obeys particular criteria. Specifically, if the reservoir has infinite specific heat and a relaxation time much shorter than that of the system, it remains in thermal equilibrium even though it interacts with a system which may not be. When these conditions are satisfied one may ignore the dynamics of the reservoir in favor of the dynamics of the system. This paradigm provides a method for calculating quantities such as equilibration time scales of a system and transition probabilities when the system is in equilibrium. In the case of Brownian motion, for example, where the system is a small macroscopic particle and the bath is the fluid in which it rests, the Langevin equation is a natural outcome of the fluctuating thermal force of the bath on the system.

In the case of field theory, however, the dichotomy of the system and bath is less clear. If there is only one self-interacting field one can decompose the dynamics into short and long-wavelength modes which operate on different time scales. The short wavelength modes respond much more quickly and can serve as the thermal bath while we define the system as those modes whose wavelengths are larger than some critical value; nonlinear interactions couple the system to the bath. Another approach is to have a second field which acts as the bath to the first field. In either case the form of the coupling determines the nature of the fluctuations which the system experiences. Below, we model the fluctuations as white noise (uncorrelated) by adding a stochastic term to the equation of motion. In general, the noise which the system experiences may be significantly more complicated, as is the case in some simple cases which have been studied [32,33]. We justify our choice by noting that it is not yet clear how these findings might change given the relatively complicated environment of the early universe. Furthermore, in at least one study [33] the authors found that in the high temperature limit the noise becomes white.

The Langevin equation is a popular way to model phenomenologically a system with thermal fluctuations, though, as mentioned above, the actual dynamics of the noise may be different from the simple model of additive white noise. Nevertheless, the crucial question is deciding how one is

going to model the essential physics of the system. Certainly, if we knew what the true equations of motion for the Higgs and particle fields were in the early universe, we could use those equations. This, however, is not the case. At the time of the electroweak phase transition, aside from the Higgs, there were many other particles, and writing the complete dynamics is, if not impossible, extremely difficult. Given this situation, using the Langevin equation with additive white noise is a reasonable place to start in the investigation of how fluctuations may affect the dynamics of the transition, and we use it here. Also, numerical studies of nucleation of critical bubbles in 1+1 and (2+1)-dimensions carried out using the Langevin equation to model thermal fluctuations have demonstrated good agreement with classical nucleation theory [34,35].

### A. The model

As described above the coupling of the field with the thermal bath is modeled by a Langevin equation. The equation of motion, then, in terms of the dimensionless variables is

$$\frac{\partial^2 \chi}{\partial t^2} = \nabla^2 \chi - \eta \frac{\partial \chi}{\partial t} - \frac{\partial V}{\partial \chi} + \xi(\mathbf{x}, t), \quad (28)$$

where we have defined  $\xi$  as the dimensionless stochastic noise. The fluctuation-dissipation theorem relates the noise to the dissipation coefficient  $\eta$  by

$$\langle \xi(\mathbf{x}, t) \xi(\mathbf{x}', t') \rangle = 2 \eta \theta \delta(t - t') \delta(\mathbf{x} - \mathbf{x}'). \quad (29)$$

In discrete form,  $\xi$  is

$$\xi(\mathbf{x}_i, t_n) = \xi_{i,n} \quad (30)$$

$$= \left( \frac{2 \eta \theta}{\delta t (\delta x)^2} \right)^{1/2} \mathcal{G}_{i,n}, \quad (31)$$

where  $\mathcal{G}_{i,n}$  is a unit variance Gaussian random number at each point on the lattice and  $\delta t$  and  $\delta x$  are the lattice spacing in the time and spatial directions, respectively. We integrate the equation of motion forward in time using a second-order leapfrog method.

We carry out the numerical experiment by inputting initial conditions and allowing the simulation to run. Since we are interested in the dynamics of the bubble wall and not questions of nucleation, we use as initial conditions a wall which stretches across the width of the lattice located at the midway point along its length. Half of the initial lattice volume, then, is in the asymmetric phase while half is in the symmetric phase. The shape of the wall is chosen so that it conforms to the kink profile appropriate for a thin wall. This profile is in fact not the one which minimizes the free energy, but it is sufficiently close so that the time it takes for the wall to relax to its correct form is much smaller than the run time. By making the wall stretch across the width of the lattice we effectively model a large bubble and thus ignore the initial expansion stage following nucleation. The wall, however, is not given any initial speed, but must accelerate to its terminal velocity. The time for this to happen is also very small.

The initial configuration of the wall is prepared without noise added in. We include the fluctuations in the simulation only through the dynamics of the equation of motion. Though such a configuration is certainly unphysical given the assumption that thermal fluctuations exist, it has no effect on the outcome of the numerical experiment. In each of the two phases there exists a thermal equilibrium distribution of the other phase due to fluctuations [2,3]. Given the strengths of the transitions we consider, the time it takes to reach this distribution is small. Only during the initial stages of the simulation is the bubble wall likely to be affected by particular characteristics of the initial conditions.

A first-order phase transition may be classified into weak and strong transitions depending on the height of the barrier separating the minima. In a weak transition considerable phase mixing may exist with the transitions proceeding through domain coarsening, while in a very strong transition we expect the theory of homogeneous nucleation and bubble expansion to be correct. We wish to explore here the intermediate region and thus must choose appropriate values for the parameters which describe the potential. Based on the findings in Ref. [2] we select values for the parameters  $\alpha$  and  $\lambda$  which explore transitions in the strong regime, where a strong transition is one where at  $\theta_c$  the symmetric phase comprises at least about 60% of the total area. We, therefore, set  $\lambda = 0.1$  and allow  $\alpha$  to take on the values 0.4 and 0.5, well into the strong regime.

The potential in Eq. (2) has a direct connection with the electroweak phase transition. In the temperature one-loop effective potential  $\alpha$  is related to the gauge-boson masses while  $\lambda$  is determined by the Higgs boson mass. The values we choose here for these parameters, however, should not be construed as exploration of the parameter space of masses of these particles. The naive interpretation that the chosen values of  $\alpha$  and  $\lambda$  correspond to masses in the minimal standard model is false in this case because the simulations describe dynamics in a (2+1)-dimensional world. What constitutes a weak and strong transition in (2+1) dimensions is different from the (3+1)-dimensional case. We choose, therefore, not to make any claims about particle masses, but rather focus qualitatively on the effects of fluctuations on the phase transition.

### B. The lattice

When taking a numerical approach to this problem one must make a choice regarding the coarse-graining scale as realized through the lattice spacing. Modes with wavelengths shorter than the lattice spacing couple to the larger wavelength modes through the noise term in the equation of motion. The results from placing the field theory on a lattice, then, only apply to the long wavelength modes. When probing physics at shorter wavelengths, one must be careful in taking the continuum limit. To do so one must include renormalization counterterms in order to obtain the proper continuum theory. These issues are discussed in more detail in Ref. [34]. Following the prescription in Ref. [2] we set the lattice spacing  $\delta x = 1$ , which is approximately equal to the mean-field correlation length given by  $l_{\text{cor}}^{-2} = V''(\chi_0, \theta_c)$ .

In addition to choosing a grid size on the lattice, one must choose the size of a time step, the size of the lattice, and the

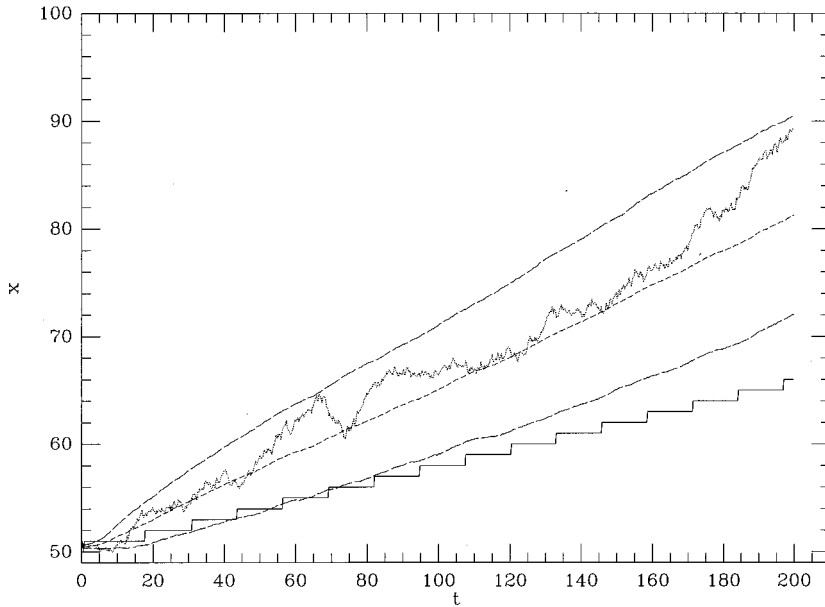


FIG. 2. Average wall position as a function of time for  $\alpha=0.4$ ,  $\eta=0.2$ . Shown are a phase transition without fluctuations (solid line), with fluctuations (dotted line), average over 200 simulations (short-dashed line), and one- $\sigma$  width (long-dashed line).

boundary conditions. Ideally a large time step would allow one to integrate the equations of motion for a longer period of time; however, stability considerations limit the size of  $\delta t$ . To find an appropriately sized step we compared simulation results as a function of different values of  $\delta t$ , choosing a value in the regime where the results become independent of the magnitude of step. In all simulations we used a value of  $\delta t=0.2$ .

As with the choice for  $\delta t$ , selecting a lattice size is another exercise in compromises. The physics one is attempting to simulate takes place in an effectively infinite volume, but one is limited to not just finite lattices but also ones which are fairly small because of the need for reasonable integration times. There are dangers, however, in having too small a lattice. Strictly speaking, in the context of phase transitions symmetry breaking only occurs in the infinite vol-

ume limit. Within any finite volume there exists the possibility that a fluctuation will restore the symmetry regardless of the dynamics internal to the volume. Since it is precisely these dynamics with which we concern ourselves, it is paramount to choose a volume large enough that the probability of such an occurrence becomes negligible. Essentially, what happens is that fluctuations in the broken phase may drive the system back to the symmetric phase, even though it is energetically unfavorable. If the total volume is large, such fluctuations result in only a small region of the total volume having its symmetry restored. The chance that this could happen with a large volume is exponentially suppressed because of the large amount of energy necessary. We can estimate how large a volume we need by calculating the rate for a large fluctuation:

$$\Gamma \sim e^{-F/\theta}. \quad (32)$$

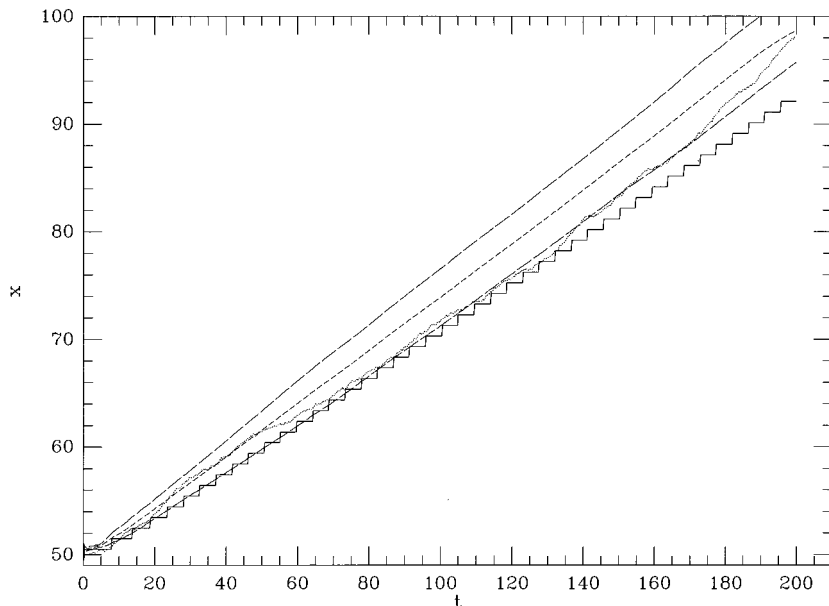


FIG. 3. As in Fig. 2 with  $\alpha=0.5$ .

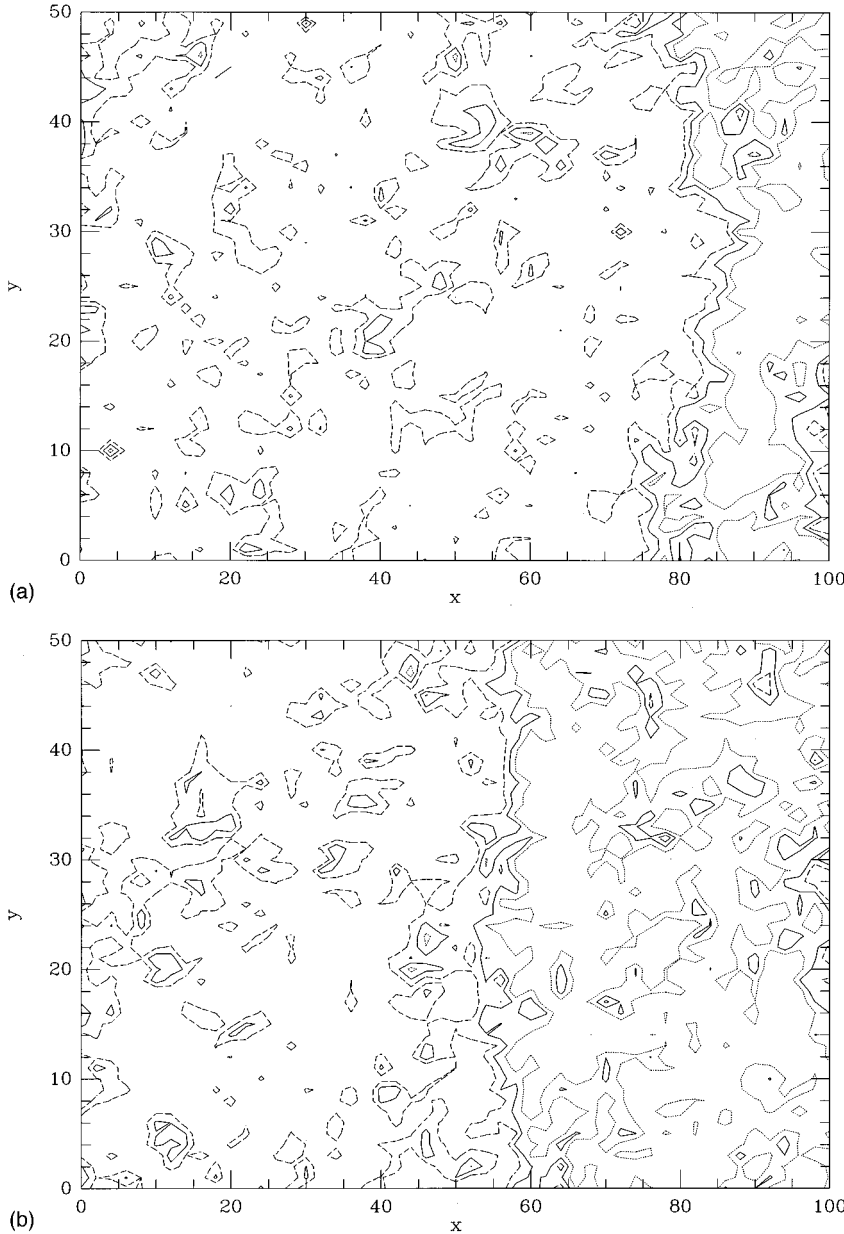


FIG. 4. Contour plot of field  $\chi$  on the lattice with contours  $\chi_-/2$  (dotted),  $\chi_-$  (solid),  $3\chi_-/2$  (dashed). (a)  $\alpha=0.4$ ,  $\eta=0.1$ . (b)  $\alpha=0.4$ ,  $\eta=0.5$ . (c)  $\alpha=0.5$ ,  $\eta=0.1$ . (d)  $\alpha=0.5$ ,  $\eta=0.1$ .

The free energy  $F$  is given by the change in effective potential energy between the two minima multiplied by the amount of volume in the asymmetric phase. Ignoring the gradient portion of the free energy, which only increases  $F$  and makes a symmetry restoring fluctuation less probable, we have

$$\frac{F}{\theta} \approx \mathcal{V} \frac{4\alpha^2 \theta_c \Delta}{9\lambda^2}, \quad (33)$$

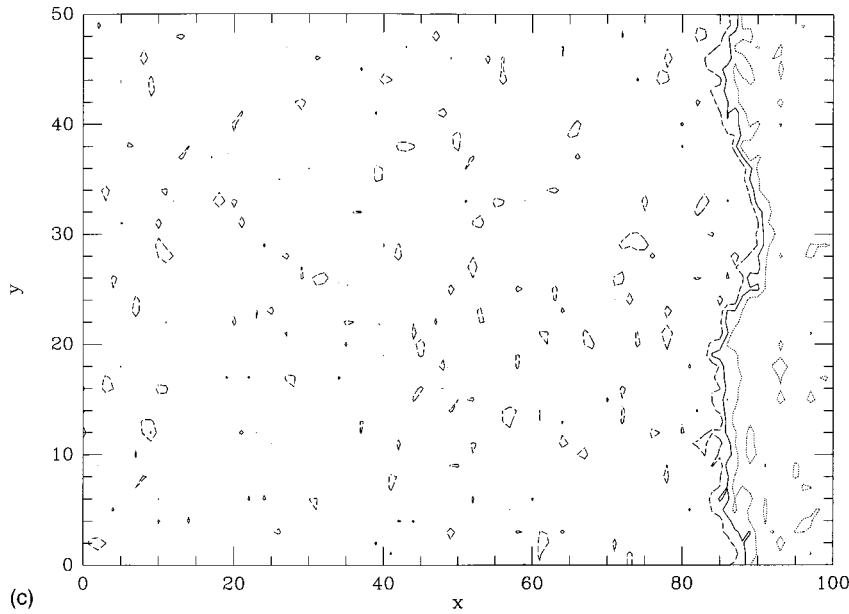
where  $\mathcal{V}$  is the volume in the symmetric phase. The probability of having a large fluctuation given the size of our lattice and run time is approximately  $10^{-10}$ .

Since we are interested in the dynamics of the bubble wall as it expands, we also want to make sure that it is unlikely that a critical bubble will nucleate in the asymmetric phase within the lattice during a run time. Because the volume under consideration is much less than a horizon volume and the time is much less than a Hubble time, the probability of

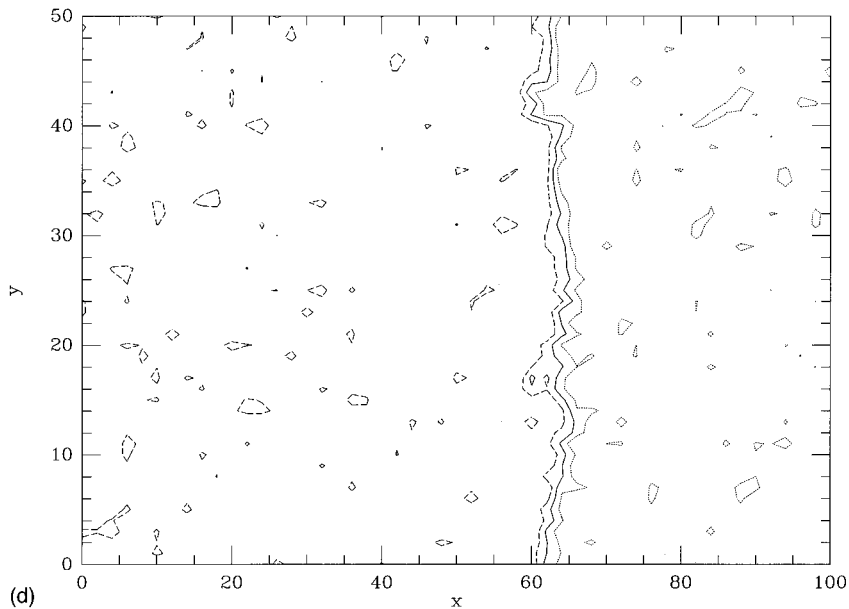
this happening is similarly suppressed. The lattice size we use in the simulations is  $L_x=100$ ,  $L_y=50$ , where  $L_x$  is the length in the  $x$  direction and  $L_y$  is the length in the  $y$  direction.

Another consideration lies in the fact that we are modeling an unbounded system by a finite volume with a boundary. Though, as discussed above, we do not expect finite size effects to be important, there is a distinct surface in the simulations which is unphysical. We circumvent this issue by using periodic boundary conditions in the  $y$  direction and ‘‘open’’ boundary conditions in the  $x$  direction. The periodic conditions allow us to model an essentially planar wall, appropriate for a large bubble. The danger, however, with periodic conditions is that long range correlations may be induced if the simulation is run for longer than  $L_y/2$ , the light crossing time. It turns out that this is not a concern here because the presence of dissipation and noise have the effect of damping out and swamping any long range ‘‘communication’’ which might otherwise exist. The open boundary con-





(c)



(d)

FIG. 4 (Continued).

ditions consist of assuming that for points immediately outside the lattice the field takes on a value equal to the field on the boundary. Though not realistic, these boundary conditions provide an approximation to the unbounded system. Any spurious effects caused by these conditions do not extend into the lattice because of dissipation and noise.

#### IV. RESULTS

The focus of the numerical experiment is to understand the effect of the fluctuations on the rate at which the old phase is converted into the new phase and how that transition is made. We expect that for a relatively stronger transition the fluctuations will play a fairly minor role, while for a relatively weak transition there may be a marked difference from the homogeneous background case. We investigate the rate of phase conversion for different transition strengths by allowing  $\alpha$  to vary while holding all other parameters con-

stant and comparing the results to the case where there are no fluctuations. The values of  $\alpha$  we choose (0.4 and 0.5) place the transition in the strong regime as defined in Ref. [2]. In that study the author found that the change from a weak to a strong transition is itself a second-order phase transition with a critical value of  $\alpha_c = 0.36$ . We can characterize the strength of the transition by  $f_+$ , the fraction of volume which fluctuates from the symmetric phase beyond the maximum of the potential barrier. At the critical value  $\alpha_c$  this fraction is 42%, while for  $\alpha = 0.4$ ,  $f_+ \approx 6\%$  and for  $\alpha = 0.5$ ,  $f_+ \approx 0.1\%$ . Furthermore, whereas in the homogeneous background case the field in a region of space smoothly makes the transition from the symmetric to asymmetric phase, we do not expect this to happen when the amplitude of the noise becomes large.

In order to calculate the rate of phase transformation for a particular transition we first introduce a definition which will allow us to determine which phase the field is in. We label the field at a particular lattice point as being in either the 0

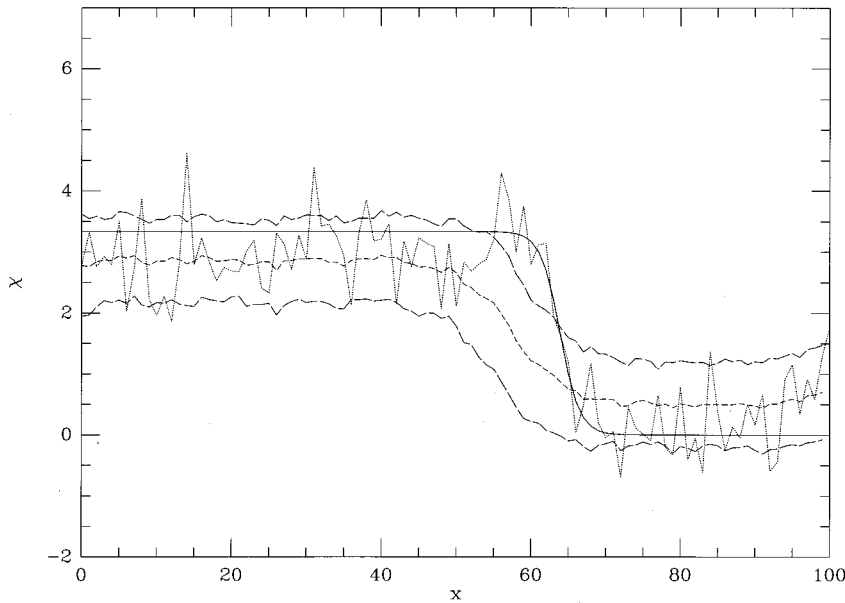


FIG. 5. Wall profile for  $\alpha=0.4$ ,  $\eta=0.1$ . Shown are simulation results for a phase transition without fluctuations (solid line), with fluctuations (dotted line), average over 200 simulations (short-dashed line), and one- $\sigma$  width (long-dashed line).

phase if  $\chi \leq \chi_-$  (i.e., to the left of the maximum) or the + phase if  $\chi > \chi_-$  (i.e., to the right of the maximum). This allows us to determine what fraction of the total volume is in each of the two phases. Because we place the bubble wall through the center of the lattice approximately half of the initial volume is in each phase with deviations away from half due to fluctuations. Lattice points move on average from the 0-phase to the + phase as the bubble expands. In Figs. 2 and 3 we plot the position of the wall as a function of time for a phase transition with and without fluctuations for  $\alpha=0.4$  and  $\alpha=0.5$  with  $\eta=0.2$ . The wall position for the case with fluctuations as shown by the short-dashed line is an ensemble average of 200 separate trials while the long-dashed lines show the one standard deviation width of the distribution. The dotted line shows one realization. The solid line is the position for a phase transition without fluctuations, where the steplike nature is due to the discreteness of the

lattice. For the case with fluctuations the position does not mean that the midpoint of the wall is located at that particular  $x$  position all the way across the lattice; rather, it represents an average position at that point in time. In fact there are regions both in front of and behind the wall which belong to the opposite phase resulting in a somewhat amorphous boundary. Figures 4(a)–4(d) show contour plots of the field on the lattice for  $\alpha=0.4$ , 0.5 with  $\eta=0.1$ , 0.5 with contours at  $\chi_-/2$  (dotted),  $\chi_-$  (solid),  $3\chi_-/2$  (dashed). We see significant distortions in the wall away from planar in the weaker transitions whereas the stronger transitions approach the plane solution, though other structure is still evident. The rate at which phase is converted from the 0 to the + state is also clearly elevated relative to the transformation without fluctuations. In Table I we show the rate of phase conversion, essentially the velocity of the wall, for the different transition parameters. The right-hand columns for a given

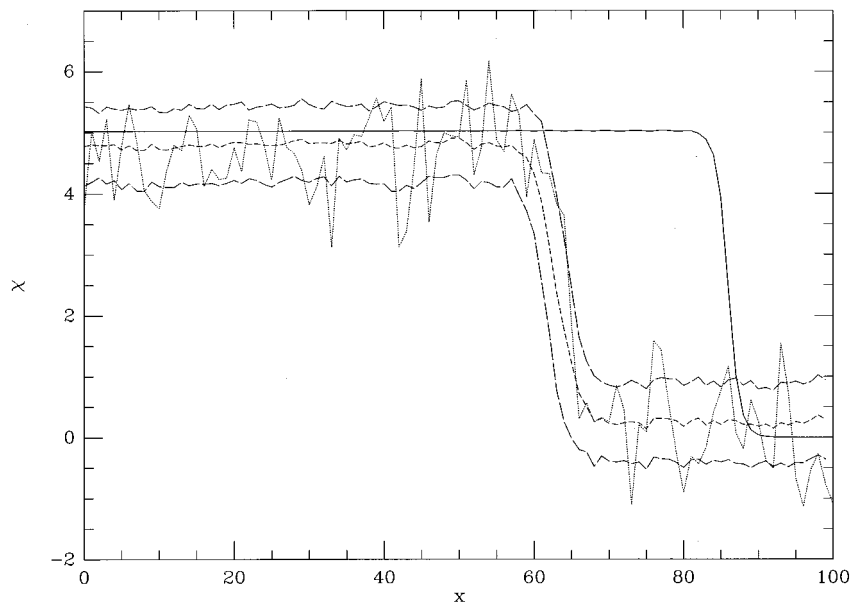


FIG. 6. As in Fig. 5 with  $\alpha=0.5$ .

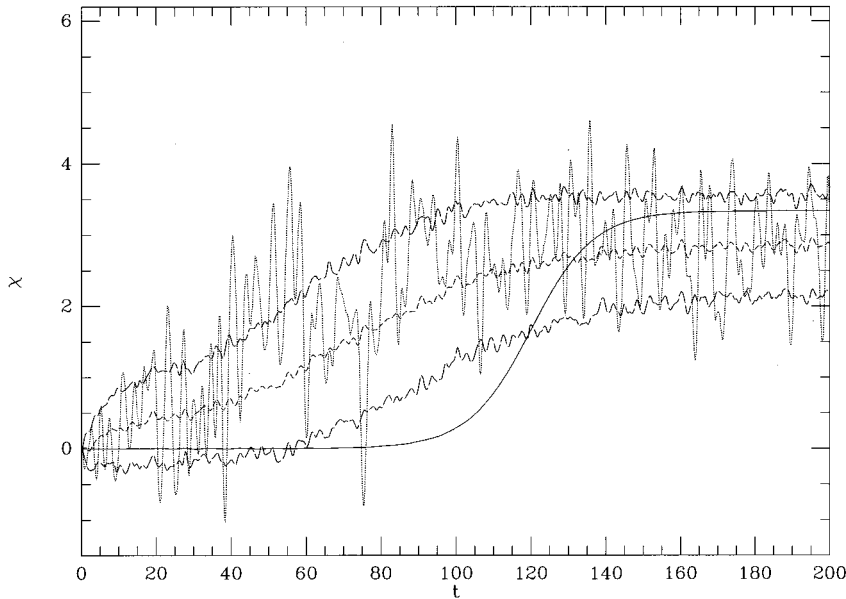


FIG. 7. Lattice point history for  $\alpha=0.4$ ,  $\eta=0.1$ . Shown are simulation results for a phase transition without fluctuations (solid line), with fluctuations (dotted line), average over 200 simulations (short-dashed line), and one- $\sigma$  width (long-dashed line).

value of  $\alpha$  and  $\eta$  show the average wall velocity for the fluctuating background case along with the one sigma width; the left-hand columns show the wall velocity for the homogeneous background case. In the limit of a very strong transition we can see that the rate of phase conversion approaches the homogeneous theory solution.

Also particularly relevant to electroweak baryogenesis is the actual structure of the wall. Whether and how many baryons are created depends on how particles, which are interacting with the changing Higgs field, make the transition from the 0 to the + state. Though this depends on quantities such as the velocity of the particle relative to the wall, which we don't calculate here, we can still get an idea of what a particle "sees" as it moves from one state to the other by taking cross sections of the wall. In Figs. 5 and 6 we plot the values of the field  $\chi$  as a function of  $x$  at a particular time for  $\alpha=0.4$  and  $\alpha=0.5$  with  $\eta=0.1$  for both the homogeneous

and fluctuating background theories. While the wall thickness in the homogeneous theory can be clearly defined, it is less apparent in the fluctuating case. We see that averaged over 200 simulations the wall is thicker relative to the case where there are no fluctuations, though the increase is only moderate for the transition strengths used here and approaches the homogeneous background solution for a stronger transition.

Figures 7 and 8 follow the behavior of a lattice point as a function of time. The boundaries of when the transition from the 0 to + state begin and end is less clear in the fluctuating case as compared to the homogeneous case. The results from averaging over many simulations indicates that in general a lattice point makes the transition more slowly than if there were no fluctuations. This results because in the vicinity of the bubble wall a lattice point may undergo several "transitions" before finally reaching equilibrium in the + phase.

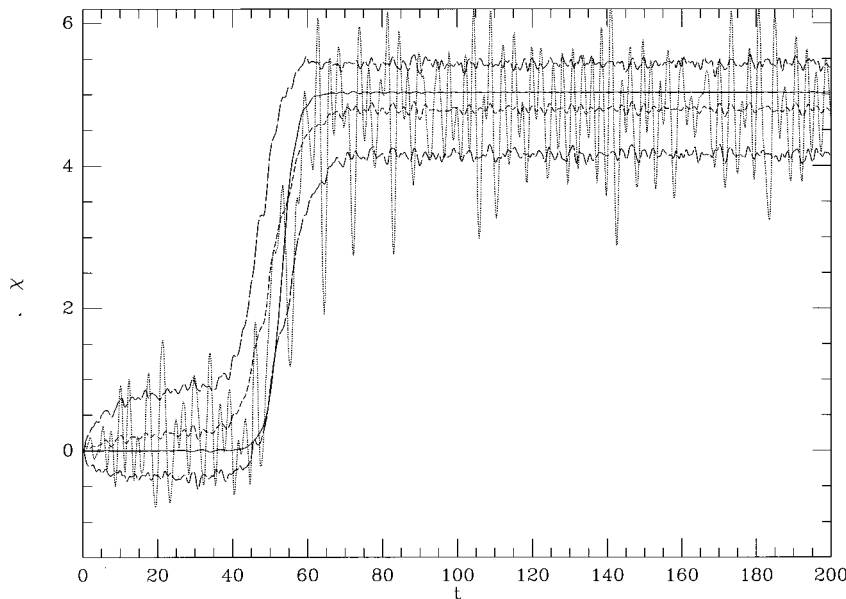


FIG. 8. As in Fig. 7 with  $\alpha=0.5$ .

TABLE I. Wall velocities for varying parameter values where  $v_h$  represents the velocity in simulations without fluctuations and  $v_f$  represents the velocity in simulations with fluctuations.

$\alpha$	$\eta=0.1$		$\eta=0.2$		$\eta=0.5$	
	$v_h$	$v_f$	$v_h$	$v_f$	$v_h$	$v_f$
0.4	0.15	$0.24 \pm 0.06$	0.08	$0.16 \pm 0.05$	0.035	$0.077 \pm 0.036$
0.5	0.4	$0.40 \pm 0.06$	0.21	$0.25 \pm 0.02$	0.09	$0.12 \pm 0.01$

## V. CONCLUSIONS

We see that quantities such as the rate of phase conversion and the structure of the bubble wall can be different for phase transitions with fluctuations as compared to the standard homogeneous background model. The speed of the bubble wall may be increased by a factor of about two for a ‘‘mildly’’ strong transition and probably even more for weaker transitions. Physically, this is a reasonable expectation; the wall effectively ‘‘swallows’’ the field fluctuations, moving forward as it does so. In a transition with more large amplitude fluctuations this swallowing effect is more pronounced. Though the rate at which phase is converted from the 0 to the + phase is increased globally, locally the transition is not necessarily well defined and more gradual. Furthermore, we see that this effect is noticeable even though only a small percentage (about 6%) of the symmetric phase may fluctuate beyond the barrier at any given time. As the amplitude of the fluctuations decrease the bubble behaves as predicted by the homogeneous background theory. That there are large amplitude fluctuations which can roughly ‘‘mask’’ the transition is not surprising; in fact, this is entirely determined by the stochastic noise term in the equation of motion. What is interesting is that the noise should have such a significant effect on a transition which one would consider ‘‘strong’’ by the definition given in Ref. [2].

It is not necessarily evident that random fluctuations should result in an increase in the velocity of the bubble wall. Though fluctuations from the 0 to + phase might speed up the wall, one might also expect that fluctuations from the + to 0 phase would have the opposite effect, resulting in no net change. It is the asymmetry in the potential, however, which prevents this from happening. Because fluctuations are a result of a random impulse on the field at a particular point, a fluctuation which drives the field from the 0 to + phase is more likely to approach or exceed the maximum of the potential than those that go from the + to 0 phase. The dominant effect on the dynamics, then, is to enhance to 0 to + transition.

The implications for baryogenesis stem from the fact that models rely on particular assumptions of the bubble wall structure, e.g., a smoothly varying monotonic order parameter. The standard picture [15] states that, depending on the thickness of the wall, one selects a mechanism with which to calculate the baryon number generated. In order for this to work, however, it is necessary that the homogeneous background theory of bubble nucleation and expansion be valid. Previous studies have called into question this paradigm by pointing out that subcritical bubbles may affect the initial conditions of the transition as well as bubble nucleation [1–6] in a weak first-order phase transition. Here we inves-

tigate transitions which are stronger than those in Ref. [2], but still within the regime where nucleation may be affected by the presence of subcritical bubbles [6]. Although the electroweak transition is most likely weak in the minimal standard model, authors [7,8,15] have argued that baryogenesis is likely only for a sufficiently strong transition where the effects of phase mixing due to thermal fluctuations would be negligible. What we have shown here is that the realm of the phase transition for which fluctuations may play a significant role is larger than what was expected. Their effect is not limited to possible alterations in the picture of homogeneous nucleation or degree of phase mixing, but also includes the dynamics subsequent to nucleation. For instance, not only are the wall thickness and velocity larger, but the path from the symmetric phase to the asymmetric phase is hardly smooth or monotonic. Any model for electroweak baryogenesis will clearly have to take the stochastic nature of the dynamics into account when considering the interaction of particles with the Higgs field. The results here are not meant to be quantitative, but they do demonstrate the importance of fluctuations in the dynamics of first- order phase transitions.

Finally, we point out some of the limitations of this work. Ultimately, we would like to be able to obtain a complete picture of the electroweak phase transition in order to determine the viability of generating the baryon asymmetry of the Universe at this scale. What we have done here is to examine the role thermal fluctuations are likely to have on the transition dynamics, and what the implications are on models of baryogenesis. However, this study was limited to (2+1) dimensions rather than the 3+1 dimensions of the real world. Extending this work to higher dimensions would be a valuable contribution to our understanding of this problem. Also, we have assumed here that one can model the thermal fluctuations through stochastic white noise, as one does when studying phenomena such as Brownian motion. Realistically, this is only an approximation of more complicated couplings between system and bath. Indeed, how one is to divide the physical environment into system and bath and the nature of the noise that results is a problem currently under active investigation [32, 33]. Lastly, the dynamics of the cosmological fluid have been omitted. Not only should the fluctuations have an effect on the fluid, but, as already noted, the fluid itself plays a role in the overall dynamics. A more complete treatment would include fluid velocity, pressure, and temperature as well as parameters for heat capacity and conductivity in the simulations. In spite of these caveats, we believe that our findings are indicative of what we may eventually find to be the ‘‘true’’ dynamics.

## ACKNOWLEDGMENTS

I would like to thank Edward Kolb, Mike Turner, Ed Blucher, and Emil Martinec for their valuable input and advice and Marcelo Gleiser for his helpful comments. M.A. was supported in part by the U.S. DOE at Chicago and by NASA Grant No. NAG 5-2788 at Fermi National Laboratory.

- [1] M. Gleiser and E. W. Kolb, Phys. Rev. Lett. **69**, 1304 (1992); G. Gelmini and M. Gleiser, Nucl. Phys. **B419**, 129 (1994); M. Gleiser, E. W. Kolb, and R. Watkins, *ibid.* **B364**, 411 (1991); N. Tetradis, Z. Phys. C **57**, 331 (1993).
- [2] M. Gleiser, Phys. Rev. Lett. **73**, 3495 (1994).
- [3] J. Borrill and M. Gleiser, Phys. Rev. D **51**, 4111 (1995).
- [4] T. Shiromizu, M. Morikawa, and J. Yokoyama, Prog. Theor. Phys. **94**, 795 (1995).
- [5] M. Gleiser, A. F. Heckler, and E. W. Kolb, Report Nos. Fermilab-Pub-95-374/A, DART-HEP-95/07, cond-mat/9512032 (unpublished).
- [6] M. Gleiser and A. F. Heckler, Phys. Rev. Lett. **76**, 180 (1996).
- [7] K. Enqvist, A. Riotto, and I. Vilja, Phys. Rev. D **52**, 5556 (1995).
- [8] M. Dine, R. G. Leigh, P. Huet, A. Linde, and D. Linde, Phys. Rev. D **46**, 550 (1992).
- [9] P. Arnold and O. Espinosa, Phys. Rev. D **47**, 3546 (1993); W. Buchmuller, Z. Fodor, and A. Hebecker, Nucl. Phys. **B447**, 317 (1995); K. Kajantie, M. Laine, K. Rummukainen, and M. Shaposhnikov, *ibid.* **B446**, 189 (1996); P. Arnold and L. Yaffe, Phys. Rev. D **49**, 3003 (1994); W. Buchmuller and O. Philipsen, Nucl. Phys. **B443**, 47 (1995); Z. Fodor and A. Hebecker, *ibid.* **B432**, 127 (1994).
- [10] B.-H. Liu, L. McLerran, and N. Turok, Phys. Rev. D **46**, 2668 (1992).
- [11] A. F. Heckler, Phys. Rev. D **51**, 405 (1995).
- [12] P. Arnold, Phys. Rev. D **48**, 1539 (1993).
- [13] G. W. Anderson and L. J. Hall, Phys. Rev. D **45**, 2685 (1992).
- [14] G. D. Moore and T. Prokopec, Phys. Rev. Lett. **75**, 777 (1995); Phys. Rev. D **52**, 7182 (1995).
- [15] A. G. Cohen, D. B. Kaplan, and A. E. Nelson, Annu. Rev. Nucl. Part. Sci. **43**, 27 (1993).
- [16] A. G. Cohen, D. B. Kaplan, and A. E. Nelson, Nucl. Phys. **B373**, 453 (1992); Phys. Rev. Lett. **B294**, 57 (1992).
- [17] V. A. Kuzmin, V. A. Rubakov, and M. E. Shaposhnikov, Phys. Lett. **155B**, 36 (1985).
- [18] L. McLerran *et al.*, Phys. Lett. B **256**, 451 (1991); M. Dine, P. Huet, and R. Singleton, Nucl. Phys. **B375**, 625 (1992); M. Dine *et al.*, Phys. Lett. B **257**, 351 (1991); A. G. Cohen and A. E. Nelson, *ibid.* **297**, 111 (1992).
- [19] D. Comelli, M. Pietroni, and A. Riotto, Phys. Lett. **B354**, 91 (1995).
- [20] A. Riotto, Phys. Rev. D **53**, 3834 (1996).
- [21] A. Sopczak, in *Particle Physics in the Nineties*, Proceedings of the Autumn School, Lisbon, Portugal, 1993, edited by G. C. Branco and M. Pimenta [Nucl. Phys. B (Proc. Suppl.) **37C**, 168 (1995)].
- [22] G. F. Mazenko, O. T. Valls, and P. Ruggiero, Phys. Rev. B **40**, 384 (1989); M. C. Cross and P. C. Hohenberg, Rev. Mod. Phys. **65**, 851 (1993); J. Armero *et al.*, Phys. Rev. Lett. **76**, 3045 (1996), and references therein.
- [23] J. Langer, Ann. Phys. (N.Y.) **54**, 258 (1969).
- [24] A. Linde, Nucl. Phys. **B216**, 421 (1983); **B223**, 544, (1983).
- [25] S. Coleman, Phys. Rev. D **15**, 2929 (1977); C. Callan and S. Coleman, *ibid.* **16**, 1762 (1977).
- [26] B. Link, Phys. Rev. Lett. **68**, 2425 (1992).
- [27] M. Kamionkowski and K. Freese, Phys. Rev. Lett. **69**, 2743 (1992).
- [28] E. W. Kolb and M. S. Turner, *The Early Universe* (Addison-Wesley, Reading, MA, 1990), Chap. 3.
- [29] P. Huet, K. Kajantie, R. G. Leigh, B. H. Liu, and L. McLerran, Phys. Rev. D **48**, 2477 (1993).
- [30] M. Abney, Phys. Rev. D **49**, 1777 (1994).
- [31] L. Rezzolla, Phys. Rev. D **54**, 1345 (1996).
- [32] D. S. Lee and D. Boyanovsky, Nucl. Phys. **B406**, 631 (1993); M. Morikawa, Phys. Rev. D **33**, 3607 (1986); B. L. Hu, J. P. Paz, and Y. Zhang, in *The Origin of Structure in the Universe*, edited by E. Gunzig and P. Nardone (Kluwer Academic, Dordrecht, 1993).
- [33] M. Gleiser and R. O. Ramos, Phys. Rev. D **50**, 2441 (1994).
- [34] M. Alford and M. Gleiser, Phys. Rev. D **48**, 2838 (1993).
- [35] F. Alexander and S. Habib, Phys. Rev. Lett. **71**, 955 (1993); M. Alford, H. Feldman, and M. Gleiser, *ibid.* **68**, 1645 (1992).